Shape coexistence in the odd-odd neutron-rich nucleus 98Y studied in the interacting boson model

Brant, Slobodan; Lhersonneau, G.; Sistemich, K.

Download date / Datum preuzimanja: **2025-03-01**

Repository / Repozitorij:

Repository of the Faculty of Science - University of Zagreb

Shape coexistence in the odd-odd neutron-rich nucleus ^{98}Y studied in the interacting boson model

S. Brant

Department of Physics, Faculty of Science, University of Zagreb, Bijenička 32, 10000 Zagreb, Croatia

G. Lhersonneau

Laboratori Nazionali di Legnaro, Viale dell'Università 2, 35020 Legnaro, Italy

K. Sistemich

Institut für Kernphysik, Forschungszentrum Jülich, 52425 Jülich, Germany

The available data on levels in ^{98}Y have been reevaluated and interpreted using recently published information on band structure in this region. A calculation in the interacting boson model framework suggests that the 1182 keV 0.8 μs isomer is a spherical 10^- state with the $\pi g_{9/2} \, \nu h_{11/2}$ configuration. This assignment implies that the 8.0 μs bandhead at 496 keV is a $I^\pi = 4^-$ state, with the highly probable $\pi[422]5/2 \, \nu[541]3/2$ configuration. The level structure of ^{98}Y is well reproduced by coupling the levels of its both spherical and deformed odd-A neighbors and the origin of the isomeric states is understood.

I. INTRODUCTION

The neutron-rich odd-odd $^{98}_{39}$Y nucleus is of particular interest owing to its position in a region where very different nuclear shapes are observed. The spherical $N=56$ subshell closure is still effective in ^{97}Y$_{58}$ [1] while, with only two more neutrons, ^{99}Y$_{60}$ has a strongly deformed ground state [2–4]. Shape coexistence in ^{98}Y has been reported. The spherical nature of the low-lying levels was proposed in a study of the β decay of ^{98}Sr to ^{98}Y [5] and was confirmed by calculations in the interacting boson fermion fermion model (IBFFM) framework [6]. It was shown that levels below 500 keV could be described by coupling the $p_{1/2}$ odd proton (the ground state of odd-mass yttrium isotopes up to ^{97}Y) with the lowest-lying spherical neutron levels of ^{97}Sr and ^{99}Zr that are the neigboring isotones ($N=59$) of ^{98}Y. The best evidence for excited deformed states is a rather regular band with the head at 496 keV which was among the very first bands observed in this region [7]. The original cascade of four transitions of 101, 130, 158, and 186 keV and their crossovers has been recently extended by the addition of two new $\Delta I=1$ transitions of 221 and 241 keV and the crossovers [8]. A K value of 2 and the odd parity have been adopted in the evaluation in Ref. [9]. However, this is in contradiction with part of the data and the structural arguments developed in Ref. [6]. The interpretation of deformed levels in ^{98}Y has long remained speculative primarily due to the poor knowledge of the deformed odd-neutron levels in ^{97}Sr and ^{99}Zr, as these nuclei could only be accessed after β decay of on-line mass-separated fission products [10–12]. Only recently, significant progress has been achieved owing to prompt-fission experiments carried out by the GAMMASPHERE and EUROBALL Collaborations [13–16].

This paper tries to clarify the situation about the levels in ^{98}Y, in particular of the deformed ones and of the μs isomers, through a IBFFM calculation. This calculation extends the previous one in Ref. [6] which was limited to low-lying spherical levels. Moreover, results of measurements carried out at the gas-filled separator JOSEF at the DIDO reactor of the Forschungszentrum Jülich/Germany, so far only available as conference proceedings [17], will be presented.

II. EXPERIMENTAL RESULTS

Transitions and levels observed in the decay of ^{98}Y μs isomers populated in thermal fission, briefly reported in Ref. [17], are listed in Tables I and II. They are shown in Fig. 1 together with the levels seen in β decay of ^{98}Sr of interest for the present analysis of the structure of ^{98}Y. We will give some details about experimental conversion coefficients and level lifetimes. More data are included in Ref. [9]. Conversion electron coefficients have been measured either by the fluorescence method (yielding α_K) or by using intensity balance arguments in gated spectra (yielding α). Level lifetimes have been measured by the delayed-coincidence method, using the centroid and slope analysis. Intrinsic Ge and Ge(Li) detectors were used for the measurement of the γ rays while the β particles were detected with thin plastic scintillators.

The time spectrum for the $\gamma(121)$-$\gamma(204)$-t coincidence events exhibits a clear slope. Figure 2 shows the spectrum with the 121 keV line starting the time-to-amplitude converter and the 204 keV line as the stop signal. Another time spectrum (not shown) is obtained when exchanging the transitions as start/stop channels. The average of the half-lives deduced from the slopes is $t_{1/2}=35.8(8)$ ns and has been adopted in Ref. [9] as the half-life of the 375 keV level. Only upper limits could be determined for the lifetimes of the levels in the rotational band. They are in accordance with the dipole character of the stop-over transitions.

The half-life of the first excited state at 119 keV was determined to be $t_{1/2}=0.14(5)$ ns [18]. The longer lifetime of about 11 ns reported in earlier works is probably a conse-

TABLE I. Transitions observed in the decay of μs isomers in ^{98}Y at the JOSEF gas-filled separator. Intensities have been corrected for the decay of the ^{98}Y ions on their way from the interior of the reactor to the exit of the separator.

E_γ (keV)	I_γ	From	To	α_K	α	Multipolarity
49.8 (3)	3.8 (9)	496	446		0.55 (25)	$E1, M1$
51.4 (1)	22 (3)	171	119	2.1 (5)		$M1+E2$
					1.9 (5)	
71.3 (2)	0.4 (1)	446	375	1.2 (6)		$(M1+E2)$
100.7 (2)	10.0 (4)	597	496			
110.8 (2)	8.2 (8)	1082	1071		0.66 (6)	$E2$
119.4 (1)	56 (6)	119	0	0.10 (1)		$M1(+E2)$
121.3 (1)	100 (4)	496	375	0.09 (1)		$(M1)$
129.7 (2)	10.1 (7)	727	597			
157.8 (2)	9.4 (11)	884	727			
170.8 (1)	116 (12)	171	0	0.10 (3)		$E2$
186.1 (2)	9.9 (10)	1071	884			
204.2 (1)	100 (1)	375	0	0.08 (2)		$E2$
230.4 (3)	0.8 (2)	727	496			
275.2 (3)	5.8 (7)	446	171			
287.5 (3)	1.8 (3)	884	597			
344.3 (3)	3.3 (4)	1071	727			

quence of the lack of selectivity of the β-γ-t coincidences used in those measurements. As a matter of fact, the 564 and 600 keV levels have measurable lifetimes and may have contributed to increase the apparent delay of the 119 keV transition. A half-life of 2.4(12)ns is measured for the 564 keV level from the γ-γ delayed coincidences of the 36 keV-145 keV and 36 keV-564 keV pairs by the centroid-shift method. The large uncertainty is due to the difficulty to determine the prompt centroid position at 36 keV. The half-life of the 600 keV level is deduced from β-γ-t coincidences using the slopes of the time spectra for the lines of 445 keV (taking into account the contribution of the 564 keV level) and 481 keV. The average value is $t_{1/2}=7.5(7)$ ns.

III. SINGLE-PARTICLE LEVELS IN THE $A=100$ REGION

The lowest-lying spherical single-particle proton levels in odd-mass yttrium isotopes are $p_{1/2}$ and $g_{9/2}$. The former is the ground state (g.s.) and the latter is an isomeric state (at 668 keV in ^{97}Y). The next excited states are the $p_{3/2}$ and $f_{5/2}$ hole states which should be the 697 and 954 keV levels in ^{97}Y. They, however, have not been definitely assigned.

The lowest spherical single-particle neutron levels are $s_{1/2}$ (g.s.) and $g_{7/2}$, the latter being the second excited state at 308 keV in ^{97}Sr and 252 keV in ^{99}Zr. In both nuclei the first excited state is a $3/2^+$ state of complex nature [19]. We note the rates of the $E2$ transitions from the $7/2^+$ to $3/2^+$ states, of 1.75(11) and 1.33(5) Weisskopf units (W.u.) for ^{97}Sr and ^{99}Zr, respectively. Above the $7/2^+$ level there is a gap of about 300 keV up to the next levels.

The lowest-lying deformed proton levels are the [422]5/2 (g.s.), [303]5/2, and [301]3/2, Nilsson orbitals. The experi-

mental levels in ^{99}Y, with a deformation of $\beta=0.39$, are the g.s. and the excited levels at 487 and 536 keV, respectively [2–4]. These levels are particle states above the large $Z=38$ deformed gap.

The lowest-lying deformed single-particle neutron levels appear near 600 keV excitation energy in the odd-N isotones of ^{98}Y, which therefore exhibit shape coexistence. The [422]3/2 orbital has been associated with the 585 keV level in ^{97}Sr and the 724 keV level in ^{99}Zr [10–14]. The [541]3/2 orbital is associated with the levels at 644 keV and 614 keV

TABLE II. Levels observed in the decay of μs isomers in ^{98}Y at the JOSEF gas-filled separator. The levels up to 496 keV inclusive are also populated in β decay of ^{98}Sr. Spins and parities between brackets are from the present analysis. Lifetimes of μs isomers and of the 119 keV first excited state are taken from Refs. [9,18]. Configurations are from the former IBFFM calculation for spherical levels [6] and the one in this work.

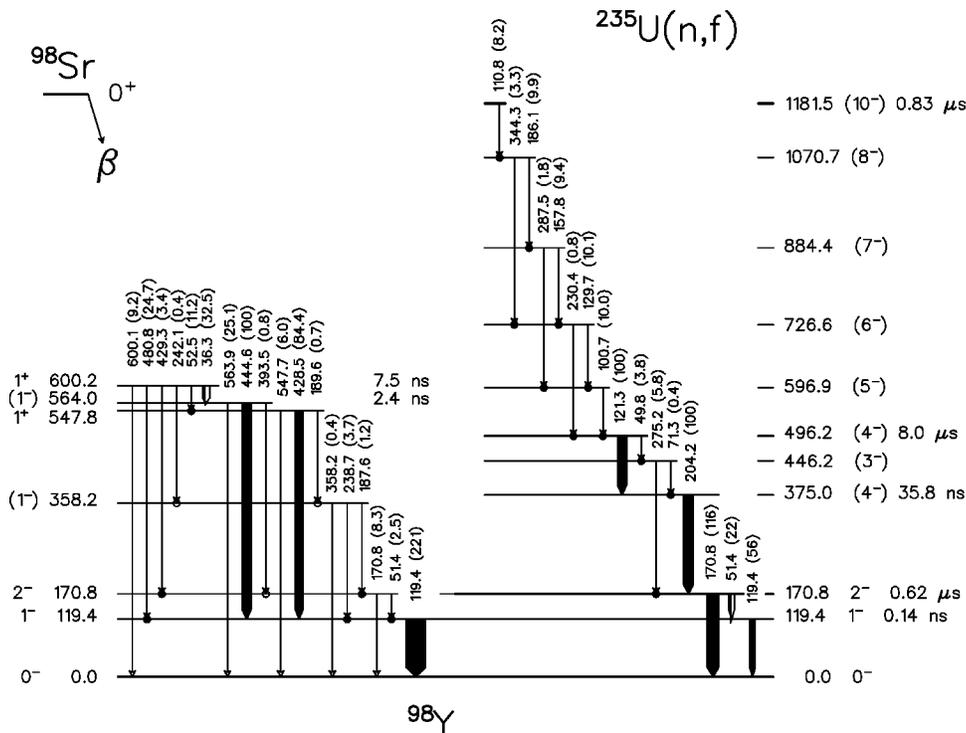| E (keV)	I^π	Half-life	Proposed configuration
0.0	0^-		$\pi p_{1/2} \, \nu s_{1/2}$
119.4 (1)	1^-	0.14(5) ns	$\pi p_{1/2} \, \nu s_{1/2}$
170.8 (1)	2^-	0.62 (8) μs	$\pi p_{1/2} \, \nu(3/2^+)$
375.0 (2)	(4^-)	35.8(8) ns	$\pi p_{1/2} \, \nu g_{7/2}$
446.2 (3)	(3^-)	<0.7 ns	$(\pi p_{1/2} \, \nu g_{7/2})$
496.2 (2)	(4^-)	8.0(2) μs	$\pi[422]5/2 \, \nu[541]3/2$
596.9 (3)	(5^-)		
726.6 (3)	(6^-)	<0.5 ns	
884.4 (3)	(7^-)	<1.0 ns	
1070.7 (3)	(8^-)	<1.5 ns	
1181.5 (4)	(10^-)	0.83(10) μs	$\pi g_{9/2} \, \nu h_{11/2}$

FIG. 1. Partial level scheme of ^{98}Y. Left-hand side: Selected information on the ^{98}Sr β-decay scheme which is of relevance in connection with this paper. Right-hand side: Complete set of levels observed in the decay of microsecond isomers populated in fission. For the level and transition energies as well as for the level half-lives the values adopted by the NDS compilation [9] are used.

in ^{97}Sr and ^{99}Zr, respectively [10,12,14]. The [404]9/2 orbital was invoked some time ago in the configurations of two-quasineutron excited states in $N=60$ isotones [2,20,21] but has been identified only very recently, first in ^{99}Zr(1039 keV) [15] and shortly later in ^{97}Sr(830 keV) [16]. The next orbitals above the Fermi surface are [411]3/2 and [532]5/2 assigned to the ground states of $N=61$ and $N=63$ isotones of Sr, Zr, and Mo [22–26].

An empirical Nilsson diagram is shown in Fig. 3. It is based on the calculation in Ref. [27] but the position of a few levels has been adjusted to qualitatively reproduce the sequence of the levels discussed above. The order of the odd-parity proton levels has been reversed and both have been slightly lowered (0.4 MeV) to more easily reproduce the $5/2^+$ ground state of $^{101}_{41}$Nb [28]. The [422]3/2 and [404]9/2 neutron orbitals have been pushed upwards and downwards, respectively, by 1.5 MeV. These shifts prevent the [404]9/2 orbital to be at the Fermi surface for $N=59$ except at the largest deformations and creates a deformation range where either the [422]3/2 or the [541]3/2 orbitals are at the Fermi surface. This scheme accounts for the observed trend of excitation energy of the $9/2^+$ state and the exchange of positions of the $3/2^+$ and $3/2^-$ levels if the deformation of ^{97}Sr is larger than the one of ^{99}Zr, as is suggested from a comparison of $B(E2)$ values for ^{98}Sr and ^{100}Zr. This crossing occurs at deformations smaller than the ones measured for $N \leqslant 60$ isotopes, in agreement with Ref. [14]. We note that pushing the [422]3/2 orbital closer to the Fermi surface was found necessary to get better agreement of the calculated energies of quasiparticle states based on it, e.g., Ref. [20].

IV. LEVELS IN ^{98}Y

Here we comment on the spin and parity of levels in ^{98}Y where we suggest deviations from the assignments in the last

evaluation of Ref. [9]. In other cases, assignments quoted in that evaluation are adopted.

A. Spherical levels

The 375 keV level is reported with $I^\pi=2^-$ in Ref. [9]. This presumably is based on the weak but still sizable population of the 375 keV level in β decay of the even-even ^{98}Sr. However, such a low spin is hardly consistent with the existence of a cascade including the $E2$ transitions of 171 keV, 204 keV and the transitions of 229 and 266 keV reported recently [8]. The $E2$ multipolarity of the 204 keV transition $(375 \rightarrow 171)$ results from the fluorescence measurement yielding $\alpha_K=0.08(2)$, see Table I. For comparison, the theoretical coefficients are $\alpha_K(M1)=0.024$, $\alpha_K(E2)=0.068$, and
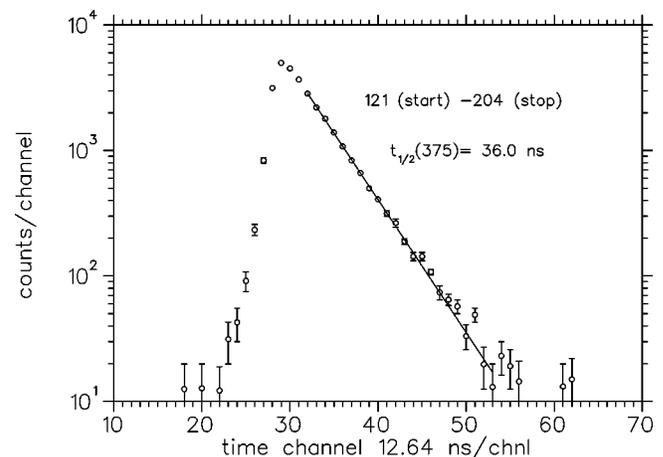

FIG. 2. The time distribution for the 121 keV-204 keV γ-γ-t coincidences showing the half-life of the 375 keV level.
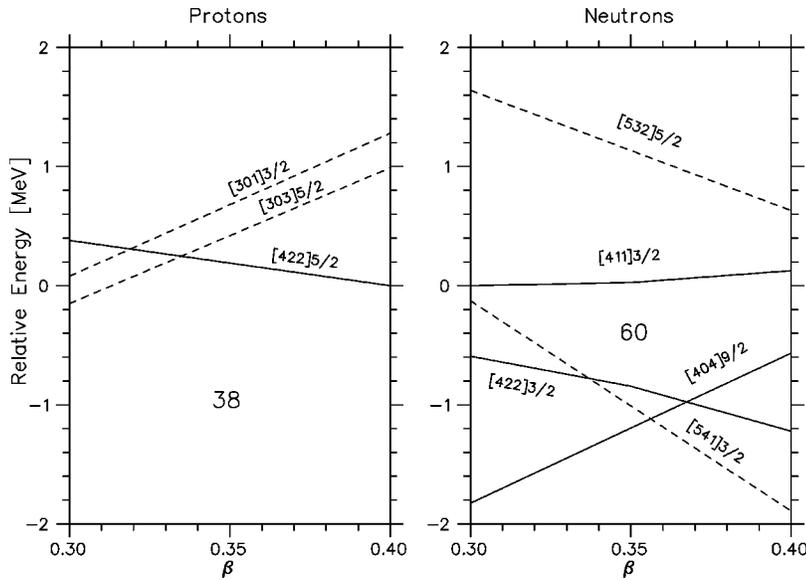
FIG. 3. Empirical Nilsson diagram for the deformed single-particle levels near the Fermi surface for ^{98}Y. See text for details.

$\alpha_K(M2)=0.136$. The smoothly increasing transition energies in the cascade, the absence of crossovers, and the $E2$ multipolarities established for the two lowest transitions suggest a stretched $\Delta I=2$ ground-state band and, consequently, $I^\pi(375)=4^-$. The decay rate of 1.7 W.u. of the 204 keV $E2$ transition creates a strong analogy with the $7/2^+$ to $3/2^+$ transitions in ^{97}Sr and ^{99}Zr. This supports the $\pi p_{1/2}\,\nu g_{7/2}$ configuration suggested in the IBFFM calculation [6].

The 446 keV level is possibly the 3^- partner (with antiparallel coupling) of the 375 keV level. The transitions to the 171 keV(2^-) and 375 keV(4^-) levels and the lack of a measurable lifetime suggest $I=3$. The conversion coefficient $\alpha =1.2(6)$ of the 71 keV transition to the 375 keV level overlaps better with $M1+E2$ [$\alpha(M1)=0.48, \alpha(E2)=3.67$] than with $E1$ [$\alpha(E1)=0.29$].

The 548 keV level (1^+ since log $ft=4.8$) has branching ratios similar to those of the 932 keV level in the spherical nucleus ^{96}Y [29]. It is thus a candidate for the $\pi g_{9/2}\,\nu g_{7/2}$ configuration.

The 1182 keV isomer [$t_{1/2}=0.8(1)$ μs] feeds the deformed band on the 496 keV level via the 111 keV transition. The total conversion coefficient $\alpha(111)=0.66(6)$ obtained by intensity balance suggests the $E2$ multipolarity [compare with $\alpha(M1)=0.14,$ $\alpha(E2)=0.73$]. The relative populations of ^{98}Y isomers in thermal-neutron fission of ^{235}U give an indication about the spin of the isomer. The 0.8 μs isomer is populated in a fraction of about 5 % of the total population of ^{98}Y. The same fraction has been measured for the high-spin isomer at 3523 keV in ^{97}Y [30] for which a three-quasiparticle configuration with $I^\pi=27/2^-$ has been proposed [1]. A spin in the range of $I=10-15$ for the 1182 keV level is therefore realistic. The *deformed* orbitals shown in Fig. 3 cannot generate a spin higher than 7. However, the IBFFM study of ^{100}Nb which is a neighboring odd-odd isotone of ^{98}Y [31] has shown that the *spherical* $(\pi g_{9/2}\,\nu g_{7/2})_{8^+}$ and $(\pi g_{9/2}\,\nu h_{11/2})_{10^-}$ configurations can create isomers in the suitable spin range.

B. Deformed levels

The 496 keV isomer [$t_{1/2}=8.0(2)$ μs] remains the lowest deformed level known in ^{98}Y and the neighboring $N=59$ isotones. The experimental conversion coefficient $\alpha_K(121,496\rightarrow375)=0.09(1)$ [while $\alpha_K(E1)=0.054, \alpha_K(M1)$ $=0.096, \alpha_K(E2)=0.44,$ and $\alpha_K(M2)=0.82$] implies a $\Delta I=1$ transition. Assuming an $E1+M2$ admixture would result in a very little hindered $M2$ rate of 0.3 W.u. that is rather improbable. The $M1+E2$ admixture is therefore favored and suggests $I^\pi(496)=(3,4,5)^-$.

The evaluation of the 496 keV level as a 2^- state in Ref. [9] has been presumably once more based on the reported direct β feeding. As a matter of fact, coincidence data obtained during a measurement dedicated to the level scheme of ^{98}Sr [20] confirm the population of the 121–204 keV cascade in the β decay of ^{98}Sr. The intensity of the 121 keV line is obtained by comparing the counts of the 121-204 and 445-119 γ-γ coincidence pairs. It is 0.6(2)% of the intensity of the 445 keV transition, in agreement with previous reports [9]. It has therefore to be assumed that part of γ feeding to the 496 keV level has escaped detection. The magnitude of this missing γ feeding requires a scenario where the intermediate and unobserved (deformed) levels do not have large branches to the low-lying (spherical) levels in spite of the larger energies available.

Another way to get insight into the nature of the 496 keV level is to consider the four band members and the $E2$ transition of 111 keV from the 0.8 μs isomer at 1182 keV to the top of the band, see Fig. 1. The spin difference of the isomer and the 496 keV level is thus six units, which according to the remarks above results in $I^\pi(496)=2^+$ or 4^-. Remembering that the dipole character of the 121 keV transition only allows $I=(3,4,5)$, these structure arguments are only consistent with $I^\pi=4^-$. The odd parity is the one experimentally favored by the conversion coefficient and the transition rate of the 121 keV transition, as noted above.

Among the levels observed in β decay of ^{98}Sr the 600 keV 1^+ level presents the best evidence for deformation.

TABLE III. Proton quasiparticle energies $\varepsilon(\pi j)$ (in MeV) and occupation probabilities $v^2(\pi j)$ used in the calculation of spherical and deformed states in ^{98}Y.

πj	Spherical		Deformed	
	$\varepsilon(\pi j)-\varepsilon(\pi p_{1/2})$	$v^2(\pi j)$	$\varepsilon(\pi j)-\varepsilon(\pi p_{1/2})$	$v^2(\pi j)$
$\pi p_{1/2}$	0	0.617		
$\pi p_{3/2}$	0.78	0.924		
$\pi f_{5/2}$	1.15	0.944		
$\pi g_{9/2}$	1.20	0.044	1.20	0.044

TABLE IV. Neutron quasiparticle energies $\varepsilon(\nu j)$ (in MeV) and occupation probabilities $v^2(\nu j)$ used in the calculation of spherical and deformed states in ^{98}Y.

νj	Spherical		Deformed	
	$\varepsilon(\nu j)-\varepsilon(\nu s_{1/2})$	$v^2(\nu j)$	$\varepsilon(\nu j)-\varepsilon(\nu s_{1/2})$	$v^2(\nu j)$
$\nu s_{1/2}$	0	0.50	0	0.48
$\nu g_{7/2}$	0.9	0.20	0.66	0.12
$\nu d_{3/2}$	1.2	0.15	0.74	0.11
$\nu h_{11/2}$	1.9	0.05	0.98	0.09
$\nu d_{5/2}$			0.98	0.92
$\nu f_{7/2}$			5.51	0.012

The 66 keV transition on top of it indicates the 666 keV level to be the probable 2^+ member of the band [5]. The experimental conversion coefficient $\alpha_K(66,666\rightarrow600)$ $=1.5(7)$, while $\alpha_K(M1)=0.52, \alpha_K(E2)=3.74$, is consistent with this interpretation. The strong β feeding of the 600 keV level (log $ft=4.1$) suggests the $(\pi[422]5/2\,\nu[422]3/2)_{1^+}$ configuration obtained by spin-flip transition of a neutron within a $\nu[422]3/2$ pair in the deformed even-even ^{98}Sr.

The 564 keV level is a low-spin level of odd parity. The parity is well established by conversion coefficients $\alpha_K(36,600\rightarrow564)=1.6(4)$ $[\alpha_K(E1)=1.74, \alpha_K(M1)=2.94]$ and $\alpha_K(445,564\rightarrow119)=0.0037(4)$ $[\alpha_K(E1)=0.0014,$ $\alpha_K(M1)=0.0034]$. The existence of a g.s. transition definitely excludes $I(564)=0$ and its large branching ratio favors $I=1$ over $I=2$. We thus assume the 564 keV level to be a 1^- state.

V. IBFFM CALCULATION FOR ^{98}Y

Models that are based on the interacting boson approximation provide a consistent description of nuclear structure phenomena in spherical, deformed, and transitional nuclei. The interacting boson model (IBM) [32,33], the interacting boson fermion model (IBFM) [34–36], and the IBFFM [37,38] are used for description of nuclear structure in even-even, odd-even, and odd-odd nuclei, respectively.

A. IBFFM description of spherical levels

The IBFFM has been previously applied in the description of spherical states in ^{98}Y [6]. Here we present the parametrization and the summary of those results. The model parameters are defined in accordance with Ref. [39] and the definition of the tensor $M1$ term is given in Ref. [40]. The spherical IBM core parameters corresponding to ^{96}Sr [31] are $h_1=0.815$ MeV, $h_2=h_3=h_{40}=0$ MeV, $h_{42}=-0.37$ MeV, $h_{44}=0.22$ MeV, with the boson number $N=4$. The proton quasiparticle energies and occupation probabilities (Table III) are similar to those for ^{96}Y [29]. The neutron quasiparticle energies and occupation probabilities (Table IV) were adjusted to ^{97}Sr [10]. In the previous calculation [6] the strengths of boson-fermion (proton) interactions for odd-parity proton configurations were adjusted to the low-lying negative parity states in ^{97}Y, while the strengths of boson-fermion (neutron) interactions for even-parity neutron configurations were taken from the calculation for low-lying positive parity states in ^{97}Sr [10]. In the present calculation

we have slightly modified the strength of the boson-fermion (neutron) dynamical interaction. The parameters for the present calculation are shown in Table V. The value of the parameter $\chi=-1.32$ has been used in the dynamical interaction and $E2$ operator. For the residual proton-neutron surface-delta and spin-spin interaction strengths we have used $V_\delta=-0.22$ MeV and $V_{\sigma\sigma}=0.2$ MeV. Using the IBFFM wave functions and the effective charges and gyromagnetic ratios: $e^\pi=1.5$, $e^\nu=0.5$, $e^{vib}=0.25$, $g_l^\pi=1$, $g_s^\pi=0.7g_s^{\pi,free}$ $=3.910$, $g_T^\pi=0$, $g_l^\nu=0$, $g_s^\nu=0.7g_s^{\nu,free}=-2.678$, g_T^ν $=\frac{1}{100}\langle r^2\rangle g_s^{\nu,free}=-0.70$, $g_R=Z/A=0.398$, the electromagnetic properties of spherical states in ^{98}Y have been calculated.

In the present calculation we have extended the fermion space by including the $\pi g_{9/2}$ according to Ref. [29] and $\nu h_{11/2}$ configurations. The strengths of boson-fermion interactions for the even parity $\pi g_{9/2}$ are different from those for negative parity proton configurations and have to be determined from calculations involving this orbital in neighboring nuclei. The values in Table V are taken from calculations for ^{97}Y [1] and ^{100}Nb [31]. The couplings of the odd parity $\nu h_{11/2}$ neutron (Table VI) are obtained from calculations for the $N=59$ isotone ^{105}Pd [41]. The extended fermion space has enabled an improved parametrization for the residual proton-neutron interaction for positive parity states in ^{98}Y: $V_T=0.034$ MeV [31] and $V_{\sigma\sigma}=0.75$ MeV, for the tensor and spin-spin interaction strengths, respectively.

The extension of the fermion space has no influence on low-energy negative parity states. It reproduces the existence of doublets based on coupling the $p_{1/2}$ proton with the g.s. and the next two excited neutron states ($s_{1/2}$, $3/2^+$ and $g_{7/2}$).

TABLE V. Strengths (in MeV) of boson-fermion (proton) monopole, dynamical and exchange interaction ($A_0^\pi, \Gamma_0^\pi, \Lambda_0^\pi$) used in the calculation of spherical and deformed states in ^{98}Y. Odd (even) proton l refers to the odd (even) orbital angular momentum of the proton that interacts with bosons.

	Spherical states		Deformed states	
	Based on odd proton l	Based on even proton l	Based on odd proton l	Based on even proton l
A_0^π		−0.25	0.02	0
Γ_0^π		0.4	0.4	0.31
Λ_0^π		0.4	2.5	17.6

TABLE VI. Strengths (in MeV) of boson-fermion (neutron) monopole, dynamical and exchange interaction ($A_0^\nu, \Gamma_0^\nu, \Lambda_0^\nu$) used in the calculation of spherical and deformed states in ^{98}Y. Odd (even) neutron l refers to the odd (even) orbital angular momentum of the neutron that interacts with bosons. The value $\Gamma_0^\nu = 0.42(*)$ refers to the calculation for positive-parity spherical states in ^{98}Y. For negative-parity spherical states $\Gamma_0^\nu = 0.62$ was used.

	Spherical states		Deformed states	
	Based on odd neutron l	Based on even neutron l	Based on odd neutron l	Based on even neutron l
A_0^ν	−0.01	0.18	0.19	0.25
Γ_0^ν	1.2	0.42 (*)	0.9	0.6
Λ_0^ν	1.4	0.4	7.0	2.5

We confirm the spin and parity assignments $0^-, 1^-, 2^-, 1^-, 4^-$ to the ground state and the excited levels at 119, 171, 358 keV (probable although experimentally not definitely established as 1^-) and 375 keV (discussed above), respectively (see Fig. 4). A detailed discussion of these levels, with wave functions and electromagnetic decay properties, can be found in Ref. [6]. At 1389 keV the present calculation predicts a 10^- state based on the $\pi g_{9/2} \nu h_{11/2}$ configuration. Below this excitation energy, the IBFFM does not predict any 8^- and 9^- state and therefore the 10^- state cannot decay to negative-parity spherical states.

The lowest positive-parity state is very probably the 5^+ level based on the $\pi g_{9/2} \nu s_{1/2}$ configuration. It should correspond to the isomeric state ($t_{1/2} = 2.0$ s) known from β decay of ^{98}Y and reported at an energy of 410(30) keV [42]. The isomeric character in spite of the lowest-lying 4^- level at 375 keV can be explained by the internal structure if the
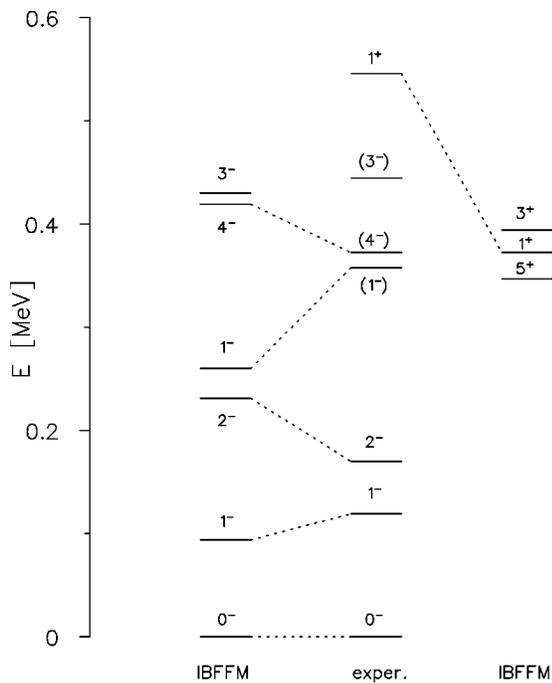

FIG. 4. Comparison of experimental spherical states in ^{98}Y with the results of the IBFFM calculation.

configurations are not very mixed. The single-particle transition changing the parity is the $\pi g_{9/2}$ to $\pi p_{1/2}$ M4 transition.

The next positive-parity states are 3^+ and 1^+ states with the respective $\pi g_{9/2} \nu d_{3/2}$ and $\pi g_{9/2} \nu g_{7/2}$ dominant components. A possible candidate for the 3^+ state is the 446 keV level. However, the experimental $\alpha_K(71)$ favors odd parity and, consequently, the $\pi p_{1/2} \nu g_{7/2}$ configuration mentioned previously. The 1^+ state is the lowest member of the $\pi g_{9/2} \nu g_{7/2}$ structure. It is associated with the experimental 548 keV level. At 1414 keV excitation energy we predict the first 8^+ state, predominantly based on the $\pi g_{9/2} \nu g_{7/2}$ configuration. This state would decay to spherical positive parity states (eight 6^+ and six 7^+ states are calculated to be below this 8^+ state). Therefore, the only candidate for the 1182 keV isomer is a 10^- level.

In conclusion to the discussion of IBFFM description of spherical levels in ^{98}Y we point out that the calculation reproduces satisfactorily the known properties of the low-lying levels below 500 keV and thus strengthens the assumption that they are of spherical nature. It is remarkable that this description is obtained with a parametrization of interaction strengths consistently derived from IBFM calculations of neighboring spherical nuclei. Although the low-lying levels in ^{98}Y seem to be very complex, the present calculation suggests that their structure is completely consistent with the systematics of spherical levels in this region. The present results may help to gain better understanding of coexistence of spherical and deformed structures at the point of rapid onset of deformation.

B. IBFFM description of deformed levels

We first use qualitative arguments based on Fig. 3 to get an insight into the deformed levels using the Nilsson terminology. The very low energy of the bandhead requires the lowest-lying orbitals in an energetically favored $K=4$ coupling. Within the valence space of Fig. 3 the only candidates are the $\pi[303]5/2 \, \nu[422]3/2$ and $\pi[422]5/2 \, \nu[541]3/2$ configurations. The $|K_p - K_n|$ partner of the 496 keV level pushed upwards by the Gallagher-Moszkowski splitting [43] is a 1^- state. It could be the 564 keV level.

In the IBFFM description first we point out to the problem of choosing the deformed core for ^{98}Y. The region of $A \approx 100$ nuclei is characterized by an extremely fast shape transition. The natural choice for the deformed core would be a deformed structure in ^{96}Sr, but there is no well established deformed band in that nucleus. A band on the second excited 0^+ level at 1465 keV with 2^+ and 4^+ band members has been proposed in Ref. [12] and is also shown by the GAMMASPHERE group [13], but was not adopted in Ref. [14] where the first excited 0^+ level at 1229 keV is shown as the head. For this reason, there is no clear prescription for choosing the deformed core in this case and therefore the nearest deformed nucleus ^{98}Sr has to be taken as the effective deformed core. The odd neutrons now are considered as holes rather than particles in respect to the boson core, as was the case for the spherical calculation.

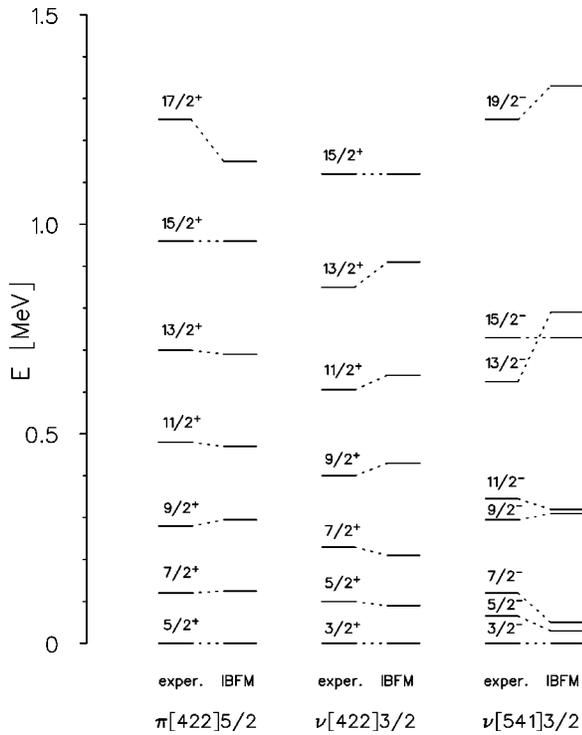Since the ^{98}Sr and ^{100}Zr nuclei are similar, the parametrization for the deformed prolate SU(3) core was taken from

FIG. 5. The experimental $\pi[422]5/2$ band in ^{99}Y [2], and the $\nu[422]3/2$ and $\nu[541]3/2$ bands in ^{97}Sr [14], compared with the results of the IBFM calculation. The energy of the lowest deformed state in each nucleus is normalized to 0 MeV. The actual energies of the $3/2^+$ and $3/2^-$ bandheads are 585 and 644 keV, respectively.

Ref. [31]: $\alpha=0.307$ MeV, $\beta=0.125$ MeV, $\chi=-1.32$ (defined in accordance with Ref. [44]), and effective boson number $N=5$. We note that some discrepancies between the present IBFFM calculation and experiment may arise due to some deviations of the boson core from the SU(3) symmetry limit. From the fit to the half-life of the first excited state in ^{98}Sr, the value of the boson charge $e^{vib}=1.9$ was derived (all other charges and gyromagnetic ratios will be taken the same as in calculations for spherical states). The relevant deformed proton configuration (the closest to the Fermi surface), namely, $\pi[422]5/2$ of $\pi g_{9/2}$ origin, was fitted to experimental data in ^{99}Y (see Fig. 5 and Tables III and V).

The neutron quasiparticle energies and occupation probabilities used in the calculation of spherical states are the best fit to experimental data that are in accordance with a series of calculations of spherical states in this mass region. For deformed states we have performed a BCS calculation that gives values rather close to those for spherical states. From the set of single-particle neutron energies: 0, 3.3, 1.9, 3.7, 3.4, 8.5 (all values in MeV) for $\nu d_{5/2}$, $\nu g_{7/2}$, $\nu s_{1/2}$, $\nu h_{11/2}$, $\nu d_{3/2}$, $\nu f_{7/2}$, and a pairing strength $G=23/A$, the quasiparticle energies and occupation probabilities have been obtained, see Table IV. The IBFM picture of bands based on $\nu[422]3/2$ and $\nu[541]3/2$ orbitals was achieved with interactions given in Table VI with $\chi=-1.32$ for positive parity configurations, and $\chi=-1.9$ for negative parity configurations, respectively (Fig. 5). We notice that IBFM cannot give

the best description of high-j low-K bands for a realistic choice of fermion energies. Therefore, the $\nu[541]3/2$ band shows some deviation from the experimental pattern, which will influence the band in the odd-odd nucleus. The present result was obtained with a χ value beyond its SU(3) limit. In this way, we have recovered part of missing correlations that allow the formation of $K \leq 3/2$ bands for a $h_{11/2}$ configuration.

From Tables V and VI we can see that there are considerable differences between the strengths of boson-fermion interactions determined for positive and negative parity fermion states, as well as between those for spherical and deformed boson cores. This is a well known fact in IBFM. In the microscopic derivation it is assumed that the origin of the boson-fermion interaction lies in the proton-neutron quadrupole interaction. In the calculation of the matrix elements all radial matrix elements are taken equal. When comparing positive and negative parity fermion states this is not a good approximation. Part of the differences also come from the fact that the proton-neutron interaction between the odd fermion and fermions in the core might be very different for different parity fermions. In microscopic calculations the strengths of boson-fermion interactions also depend on the number of single-particle configurations used in the calculation. The differences between interaction strengths for spherical and deformed cores are the simple consequence of different internal structures of spherical and deformed bosons.

The strengths of the exchange interaction Λ_0 for deformed states based on unique parity $\pi g_{9/2}$ and $\nu h_{11/2}$ orbitals (17.6 and 7.0 MeV, respectively) are not anomalously large. The deduced strengths can be compared to the values for unique parity orbitals in typical deformed nuclei in other parts of the chart of nuclides. Instead of comparing Λ_0, it is better to compare the total interaction strength Λ_{jj}^j [45]. In the present calculation the values (in MeV) of the total boson-fermion exchange interaction strength are -4.04 and -3.46 (for $\pi g_{9/2}$ and $\nu h_{11/2}$, respectively). They have to be compared to -5.48 in ^{151}Pm [45], -2.00 in ^{181}Re [46] and -4.33 in ^{181}Os [46], i.e., they are typical for deformed nuclei.

In the final step we have performed the IBFFM calculation for deformed states in ^{98}Y, where only the strength of the tensor residual proton-neutron interaction had to be determined as $V_T=-0.04$ MeV.

The calculation reproduces a band with a 4^- head. Although, due to reasons given above, the calculated deformed band does not follow the almost rotational experimental pattern, it can be with high probability assigned as $\pi[422]5/2 \, \nu[541]3/2 \, K=4^-$ band (Fig. 6, Table VII). Therefore, the experimental highest member of this band is $I=8^-$, with the same fermion, but different boson structure as the spherical $I=10^-$ level. This allows the 111 keV $E2$ transition with a rate of 1.5 Weisskopf units. The IBFFM calculates a $I=1^-$ slightly above the 4^- bandhead probably corresponding to the level at 564 keV.

One of the most appealing results is the prediction of a $I=3^-$ deformed level few keV below the $I=4^-$ bandhead. It is unclear whether it is or not the 446 keV level already discussed as being spherical. One could also consider the 496 keV level, $I=3$ being allowed by $\alpha_K(121)$, whereas the
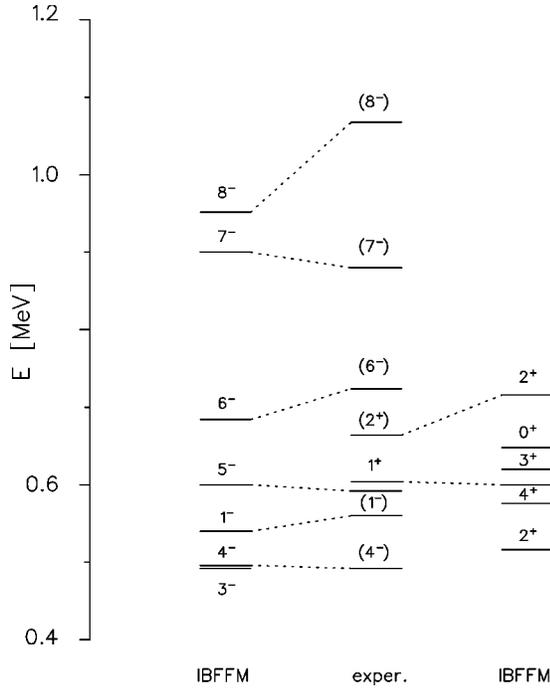
FIG. 6. Comparison of experimental deformed states in ^{98}Y with the results of the IBFFM calculation. At higher excitation energies only those theoretical states that have an experimental counterpart are shown.

4$^-$ bandhead would be slightly above at an energy of 496 $+x$. The coincidence data still could be explained if a connection via a low-energy 4$^- \rightarrow$ 3$^-$ transition would take place. Since such a transition has not been observed its energy x would have to be below the yttrium K_α x-ray energy of 15 keV. In this way, the too large β feeding of the 496 keV

TABLE VII. The electromagnetic properties of states in the deformed K=4$^-$ band in ^{98}Y. The first column identifies the transitions by their initial and final spin and parity assignments. The second and third columns contain the $B(E2)$ and $B(M1)$ values calculated in the IBFFM model. The correspondence between theoretical and experimental states is in accordance with Fig. 6. The experimental and the calculated branching ratios are displayed in the last two columns.

| | IBFFM | | I_γ | |
Transition	$B(E2)(e^2 \text{ b}^2)$	$B(M1)$ (μ_N^2)	Expt.	IBFFM
5$^- \rightarrow$ 4$^-$	0.1143	0.7180	100	100
6$^- \rightarrow$ 5$^-$	0.1164	1.0405	100	100
6$^- \rightarrow$ 4$^-$	0.1506		8	3
7$^- \rightarrow$ 6$^-$	0.1261	0.3724	100	100
7$^- \rightarrow$ 5$^-$	0.2006		19	19
8$^- \rightarrow$ 7$^-$	0.0746	0.9005	100	100
8$^- \rightarrow$ 6$^-$	0.2302		30	13

level, if a 3$^-$ state is considered instead of a 4$^-$, would be easier to account for. The existence of two closely lying levels connected via a dipole transition is not exceptional in this region. The 13 μs isomer at 420 keV in the odd-odd ^{100}Nb$_{59}$, another isotone of ^{98}Y, only decays by a 28 keV transition [47]. Unfortunately, the spin and parities of the involved levels are unknown.

We note that the deformed band structure has been reproduced without including the $g_{9/2}$ neutron in the valence space, showing that the [404]9/2 orbital plays a less important part than it had been postulated in former attempts.

Among the lowest positive parity deformed states, the IBFFM reproduces the 1$^+$ and the 2$^+$ states, corresponding to the experimental deformed levels at 600 and 666 keV, respectively. The calculation predicts a strong 0.27 W.u. $M1$ transition between them, in excellent agreement with the branching ratio of 90% of the 66 keV transition (the other decay branch is a 102 keV transition to the 564 keV level). The calculated transitions from the 1$^+$ and 2$^+$ deformed states to the 4$^+$ and 2$^+$ deformed states, predicted at excitation energies below 600 keV, are extremely weak. This is consistent with the fact that no such transitions have been observed.

The interpretation of deformed levels in ^{98}Y has long remained speculative. In conclusion to the discussion of IBFFM calculation of deformed levels in ^{98}Y we notice that the present calculation tries to clarify the structure of those levels and to give them spin and parity assignments. We have applied a procedure that consistently adopts boson-fermion interaction strengths derived from the nearest deformed odd-A nuclei, as well as the knowledge of the IBM structure of nearest deformed even-even nuclei. Such a treatment gives confidence that the interpretation of the structure of deformed levels in ^{98}Y is realistic.

VI. CONCLUSION

Results of experimental studies carried out at the gas-filled separator JOSEF and of a new analysis of the level structure of ^{98}Y are presented. A IBFFM calculation has been carried out that extends a former calculation of low-lying spherical levels of ^{98}Y to spherical levels of higher spins and deformed levels. The calculation predicts a spherical 10$^-$ isomer identified with the 1182 keV level with $t_{1/2}$=0.83 μs. The 2 s isomer near 400 keV is a 5$^+$ state with the $\pi g_{9/2}\ \nu s_{1/2}$ configuration. For the calculation of deformed levels a first stage has been a IBFM calculation for the 5/2$^+$ g.s. band of ^{99}Y and for the recently extended 3/2$^+$ and 3/2$^-$ bands in the N=59 isotones ^{97}Sr and ^{99}Zr. The IBFFM reproduces the band structure observed on the 496 keV level as K^π=4$^-$ and predicts other deformed levels that are identified with the levels at 564 keV(1$^-$), 600 keV(1$^+$), and 666 keV(2$^+$). A last feature deserving further attention is that the calculation predicts a 3$^-$ level very close to the 4$^-$ bandhead and systematically below it. This level could provide the answer why the 121 keV transition is observed in the β decay of ^{98}Sr. As a conclusion, the present calculation for the odd-odd nucleus ^{98}Y is the result of a consistent description of ^{98}Y and of its neighbors performed in the IBM framework.

[1] G. Lhersonneau, S. Brant, V. Paar, and D. Vretenar, Phys. Rev. C **57**, 681 (1998).

[2] R. A. Meyer, E. Monnand, J. A. Pinston, F. Schussler, I. Ragnarsson, B. Pfeiffer, H. Lawin, G. Lhersonneau, T. Seo, and K. Sistemich, Nucl. Phys. **A439**, 510 (1985).

[3] H. Mach, F. K. Wohn, M. Moszynski, R. L. Gill, and R. F. Casten, Phys. Rev. C **41**, 1141 (1990).

[4] F. K. Wohn, H. Mach, M. Moszynski, R. L. Gill, and R. F. Casten, Nucl. Phys. **A505**, 141 (1990).

[5] H. Mach and R. L. Gill, Phys. Rev. C **36**, 2721 (1987).

[6] S. Brant, V. Paar, G. Lhersonneau, O. W. B. Schult, H. Seyfarth, and K. Sistemich, Z. Phys. A **334**, 517 (1989).

[7] J. W. Grüter, K. Sistemich, P. Armbruster, J. Eidens, and H. Lawin, Phys. Lett. **33B**, 474 (1970).

[8] J. K. Hwang, A. V. Ramayya, J. Gilat, J . H. Hamilton, L. K. Peker, J. O. Rasmussen, J. Kormicki, T. N. Ginter, B .R. S. Babu, C. J. Beyer, E. F. Jones, R. Donangelo, S. J. Zhu, H. C. Griffin, G. M. Ter-Akopyan, Yu. Ts. Oganessian, A. V. Daniel, W. C. Ma, P. G. Varmette, J. D. Cole, R. Aryaeinejad, M. W. Drigert, and M. A. Stoyer, Phys. Rev. C **58**, 3252 (1998).

[9] B. Singh and Z. Hu, Nucl. Data Sheets **98**, 335 (2003).

[10] G. Lhersonneau, B. Pfeiffer, K.-L. Kratz, H. Ohm, K. Sistemich, S. Brant, and V. Paar, Z. Phys. A **337**, 149 (1990).

[11] M. Büscher, R. F. Casten, R. L. Gill, R. Schuhmann, J. A. Winger, H. Mach, M. Moszynski, and K. Sistemich, Phys. Rev. C **41**, 1115 (1990).

[12] G. Lhersonneau, B. Pfeiffer, K.-L. Kratz, J. Äystö, T. Enqvist, P. P. Jauho, A. Jokinen, J. Kantele, M. Leino, J. M. Parmonen, and H. Penttilä, Phys. Rev. C **49**, 1379 (1994).

[13] J. H. Hamilton, A. V. Ramayya, S. J. Zhu, G. M. Ter-Akopian, Yu. Oganessian, J. D. Cole, J. O. Rasmussen, and M. A. Stoyer, Prog. Part. Nucl. Phys. **35**, 635 (1995).

[14] W. Urban, J. L. Durell, A. G. Smith, W. R. Phillips, M. A. Jones, B. J. Varley, T. Rząca-Urban, I. Ahmad, L. R. Morss, M. Bentaleb, and N. Schulz, Nucl. Phys. **A689**, 605 (2001).

[15] W. Urban, J. A. Pinston, T. Rząca-Urban, A. Zlomaiec, G. Simpson, J. L. Durell, W. R. Phillips, A. G. Smith, B. J. Varley, I. Ahmad, L. R. Morss, and N. Schulz, Eur. Phys. J. A **16**, 11 (2003).

[16] J. K. Hwang, A. V. Ramayya, J. H. Hamilton, D. Fong, C. J. Beyer, P. M. Gore, Y. X. Luo, J. O. Rasmussen, S. C. Wu, I. Y. Lee, C. M. Folden III, P. Fallon, P. Zielinski, K. E. Gregorich, A. O. Machiavelli, M. A. Stoyer, S. J. Asztalos, T. N. Ginter, S. J. Zhu, J. D. Cole, G. M. Ter Akopian, Yu. Oganessian, and R. Donangelo, Phys. Rev. C **67**, 054304 (2003).

[17] G. Lhersonneau, R. A. Meyer, K. Sistemich, H. P. Kohl, H. Lawin, G. Menzen, H. Ohm, T. Seo, and D. Weiler, in Proceedings of the American Chemical Society Symposium on Nuclei Off the Line of Stability, Chicago, 1985, edited by R. A. Meyer and D. S. Brenner, ACS Sr. 324, Washington, 1986, p. 202.

[18] H. Ohm, G. Lhersonneau, K. Sistemich, B. Pfeiffer, and K.-L. Kratz, Z. Phys. A **327**, 483 (1987).

[19] S. Brant, V. Paar, and A. Wolf, Phys. Rev. C **58**, 1349 (1998).

[20] G. Lhersonneau, B. Pfeiffer, R. Capote, J. M. Quesada, H. Gabelmann, K.-L-. Kratz, and ISOLDE Collaboration, Phys. Rev. C **65**, 024318 (2002).

[21] J. L. Durell, W. R. Phillips, C. J. Pearson, J. A. Shannon, W. Urban, B. J. Varley, N. Rowley, K. Jain, I. Ahmad, C. J. Lister, L. R. Morss, K. L. Nash, C. W. Williams, N. Schulz, E. Lubkiewicz, and M. Bentaleb, Phys. Rev. C **52**, R2306 (1995).

[22] B. Pfeiffer, E. Monnand, J. A. Pinston, J. Münzel, P. Möller, J. Krumlinde, W. Ziegert, and K.-L. Kratz, Z. Phys. A **317**, 123 (1984).

[23] G. Lhersonneau, H. Gabelmann, M. Liang, B. Pfeiffer, K.-L. Kratz, H. Ohm, and ISOLDE Collaboration, Phys. Rev. C **51**, 1211 (1995).

[24] G. Lhersonneau, H. Gabelmann, B. Pfeiffer, K.-L. Kratz, and ISOLDE-Collaboration, Z. Phys. A **352**, 293 (1995).

[25] G. Lhersonneau, P. Dendooven, A. Honkanen, M. Huhta, M. Oinonen, H. Penttilä, J. Äystö, J. Kurpeta, J. R. Persson, and A. Popov, Phys. Rev. C **54**, 1592 (1996).

[26] M. C. A. Hotchkis, J. L. Durell, J. B. Fitzgerald, A. S. Mowbray, W. R. Philips, I. Ahmad, M. Carpenter, R .V.F. Janssens, T. L. Khoo, E. F. Moore, L. Morss, Ph. Benet, and D. Ye, Nucl. Phys. **A530**, 111 (1991).

[27] G. Lhersonneau, H. Gabelmann, N. Kaffrell, K.-L. Kratz, B. Pfeiffer, K. Heyde, and ISOLDE Collaboration, Z. Phys. A **337**, 143 (1990).

[28] H. Ohm, M. Liang, U. Paffrath, B. De Sutter, K. Sistemich, A.-M. Schmitt, N. Kaffrell, N. Trautmann, T. Seo, K. Shizuma, G. Molńar, K. Kawade, and R. A. Meyer, Z. Phys. A **340**, 5 (1991).

[29] S. Brant, G. Lhersonneau, M. L. Stolzenwald, K. Sistemich, and V. Paar, Z. Phys. A **329**, 301 (1988).

[30] G. Lhersonneau, D. Weiler, P. Kohl, H. Ohm, K. Sistemich, and R. A. Meyer, Z. Phys. A **323**, 59 (1986).

[31] G. Lhersonneau, S. Brant, and V. Paar, Phys. Rev. C **62**, 044304 (2000).

[32] F. Iachello and A. Arima, *The Interacting Boson Model* (Cambridge University Press, Cambridge, 1987).

[33] A. Arima and F. Iachello, Phys. Rev. Lett. **35**, 157 (1975); Ann. Phys. (N.Y.) **99**, 233 (1976); **111**, 201 (1978); **123**, 468 (1979).

[34] F. Iachello and O. Scholten, Phys. Rev. Lett. **43**, 679 (1979).

[35] F. Iachello and P. Van Isacker, *The Interacting Boson Fermion Model* (Cambridge University Press, Cambridge, 1991).

[36] O. Scholten, Prog. Part. Nucl. Phys. **14**, 189 (1985).

[37] V. Paar, in *Capture Gamma-Ray Spectroscopy and Related Topics—1984*, edited by S. Raman, AIP Conf. Proc. No. 125 (AIP, New York, 1985), p. 70.

[38] S. Brant, V. Paar, and D. Vretenar, Z. Phys. A **319**, 355

(1984); V. Paar, D. K. Sunko, and D. Vretenar, *ibid.* **327**, 291 (1987).

[39] Y. Tokunaga, H. Seyfarth, O. W. B. Schult, S. Brant, V. Paar, D. Vretenar, H .G. Börner, G. Barreau, H. Faust, Ch. Hofmeyr, K. Schreckenbach, and R. A. Meyer, Nucl. Phys. **A430**, 269 (1984).

[40] V. Paar and S. Brant, Phys. Lett. **74B**, 297 (1978).

[41] R. A. Meyer, S. V. Jackson, S. Brant, and V. Paar, Phys. Rev. C **54**, 2935 (1996).

[42] G. Audi, O. Bersillon, J. Blachot, and A. H. Wapstra, Nucl.

Phys. **A624**, 1 (1997).

[43] C. J. Gallagher, Jr. and S. A. Moszkowski, Phys. Rev. **111**, 1282 (1958).

[44] V. Paar, S. Brant, L. F. Canto, G. Leander, and M. Vouk, Nucl. Phys. **A378**, 41 (1982).

[45] O. Scholten and T. Ozzello, Nucl. Phys. **A424**, 221 (1984).

[46] W.-T. Chou, Wm. C. McHarris, and O. Scholten, Phys. Rev. C **37**, 2834 (1988).

[47] J. Genevey, F. Ibrahim, J. A. Pinston, H. Faust, T. Friedrichs, M. Gross, and S. Oberstedt, Phys. Rev. C **59**, 82 (1999).